ЖУРНАЛ СТРУКТУРНОЙ ХИМИИ

2017. Том 58, № 3 *Март – апрель* *С. 490 – 498*

UDC 541.6:547.021

QUANTUM MECHANICAL STUDY OF CARBON NANOTUBES FUNCTIONALIZED WITH DRUG GENTAMICIN

A. Mansoorinasab[1,2], Ali Morsali[1,2], M.M. Heravi[1,2], S.A. Beyramabadi[1,2]

[1]*Department of Chemistry, Mashhad Branch, Islamic Azad University, Mashhad, Iran*
E-mail: almorsali@yahoo.com; morsali@mshdiau.ac.ir
[2]*Research Center for Animal Development Applied Biology, Mashhad Branch, Islamic Azad University, Mashhad, Iran*

Received October, 3, 2015 *Revised February, 7, 2016*

In this work, using quantum mechanics, the noncovalent interactions and two mechanisms of covalent functionalization of drug gentamicin with (5, 5) COOH and COCl functionalized carbon nanotubes are studied. All of the calculations are performed using a hybrid density functional method (UB3LYP) in the solution phase. Quantum molecular descriptors for four possible modes of the noncovalent interaction are investigated. It is found that the binding of gentamicin with COOH (NCOOH) and COCl (NCOCl) functionalized carbon nanotubes is thermodynamically favorable. Among NCOOH and NCOCl, the first one has higher binding energy and can act as a suitable system for the drug gentamicin delivery within biological systems (noncovalent). COOH and COCl functionalized carbon nanotubes can bond to gentamicin via OH (COOH mechanism) and Cl (COCl mechanism) groups, respectively. The activation energies of four pathways in two mechanisms are calculated and compared with each other. It is specified that the COOH mechanism has an energy barrier higher than that of the COCl mechanism, being the reason for the suitability of the COCl mechanism for covalent functionalization.

DOI: 10.15372/JSC20170306

K e y w o r d s: density functional theory, gentamicin, quantum molecular descriptors, functionalized carbon nanotubes, reaction mechanisms.

INTRODUCTION

Gentamicin is a commonly used antibiotic that prevents bacterial infection around the implant. It is an aminoglycoside antibiotic, and can treat many types of bacterial infections, particularly a gram-negative infection. It is also one of the few heat-stable antibiotics that remains active even after autoclaving, and this makes it particularly useful in the preparation of certain microbiological growth media [1].

The rapid development of nanoscience has opened new ways in timely and prompt diagnosis of diseases and drug delivery. The use of carbon nanotubes in the drug delivery is a new field which is rapidly developing. So far, different systems such as polymers, dendrimers, and liposomes have been used for the drug delivery [2—4], but carbon nanotubes provide more effective structures due to high drug loading capacities and good cell penetration qualities [5].

Although the toxicity and low solubility create limitations in the applicability of carbon nanotubes, numerous laboratory-wise reports concerning the use of carbon nanotubes as the carrier molecules for drugs have been presented. A major portion of researches in this field, at both theoretical and experimental levels, has been allocated to the analysis of the possibility of adsorption of drugs and

similar compounds onto the sidewall of carbon nanotubes without considerable disfunction in its electronic structures [6—10].

Also, the interaction of carbon nanotubes with organic and aromatic molecules through covalent and noncovalent functionalization has been investigated [11—18]. The main motive behind such investigations has been the improvement of their solubility and dispersability in aqueous and organic solvents. Li et al. investigated the effect of COOH functionalized carbon nanotubes added into bullfrog collagen hydrogel on the gentamicin sulfate release [19].

In spite of the extensive use of carbon nanotubes in the drug delivery, the molecular mechanism of covalent functionalization of drugs onto COOH and COCl functionalized carbon nanotubes has not been investigated so far. In this work, using density functional theory (DFT), the covalent and noncovalent functionalization of gentamicin onto COOH and COCl functionalized carbon nanotubes was studied.

RESULTS AND DISCUSSION

Gentamicin is a non-planar molecule with the amino and hydroxyl groups protruding out of the molecular plane, as shown in Fig. 1. The optimized geometries of gentamicin (GEN), COOH (NCOOH) and COCl (NCOCl) functionalized single wall carbon nanotubes (SWCNTs) in the solution phase are shown in Fig. 1.

Gentamicin may interact with NCOOH and NCOCl through amino and hyroxyl groups to form hydrogen bonds. These four reactants (R) are shown in Fig. 2, namely, RNCOOH/OH, RNCOOH/NH, RNCOCl/OH, and RNCOCl/NH.

The binding energies (ΔE) of gentamicin with NCOOH and NCOCl were calculated using the following equation and presented in Table 1:

$$\Delta E = E_{\text{RNCOOH(RNCOCl)/OH(NH)}} - (E_{\text{NCOOH(NCOCl)}} + E_{\text{GEN}}). \quad (1)$$

According to the calculated binding energies of four configurations in Table 1, these energies are negative in the solution phase indicating that gentamicin is stabilized by NCOOH and NCOCl surfaces. Among the four configurations, the configurations related to NCOOH are more stable than the NCOCl configurations. Among the two configurations of RNCOOH/OH and RNCOOH/NH, the second one has a higher negative energy, denoting a stronger interaction. Generally, a comparison between COOH and COCl functionalized SWCNTs shows that the use of the first one is more desirable due to a stronger interaction between gentamicin and SWCNT. It was for this reason that COOH functionalized SWCNT was used for gentamicin drugs from the applicability point of view [19].

In describing the stability and chemical reactivity of different systems, quantum molecular descriptors, such as the chemical potential, the global hardness, the electrophilicity index, etc. have been used.

Table 1

Quantum molecular descriptors (eV) *and binding energies* (kJ·mol^{-1}) *for the optimized geometries of gentamicin*, COOH (COCl) *functionalized* SWCNTs, RNCOOH/OH (NH) *and* RNCOCl/OH (NH) *in the solution phase*

Species	E_{HOMO}	E_{LUMO}	E_{g}	η	μ	ω	ΔE
GEN	–5.95	–1.85	7.80	2.05	–3.90	3.70	—
NCOOH	–4.04	–2.74	1.30	0.65	–3.39	8.86	—
NCOCl	–4.08	–2.83	1.26	0.63	–3.45	9.50	—
RNCOOH/OH	–4.03	–2.73	1.30	0.65	–3.38	8.76	–36.96
RNCOOH/NH	–4.00	–2.69	1.32	0.66	–3.34	8.50	–67.40
RNCOCl/OH	–4.07	–2.80	1.27	0.63	–3.44	9.32	–13.87
RNCOCl/NH	–5.76	1.42	1.26	0.63	–3.45	9.45	–4.59

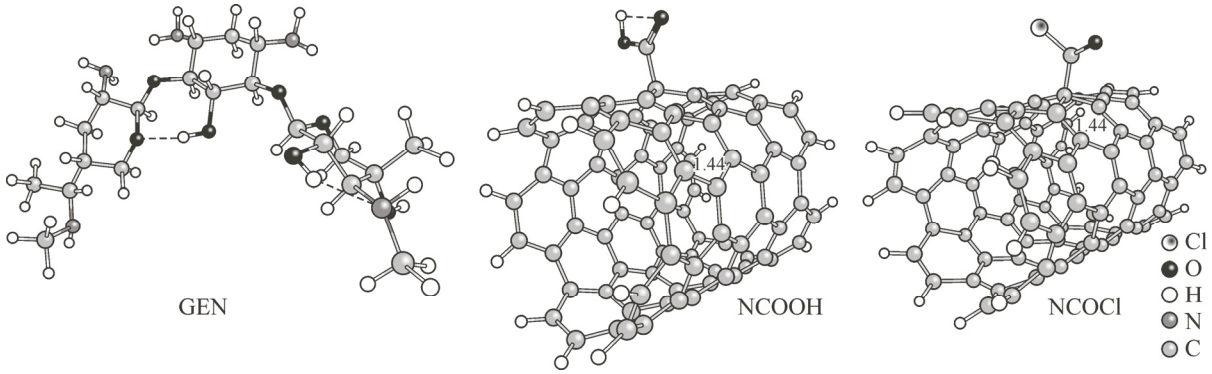

Fig. 1. Optimized structures of gentamicin (GEN), COOH (NCOOH) and COCl (NCOCl) functionalized SWCNTs

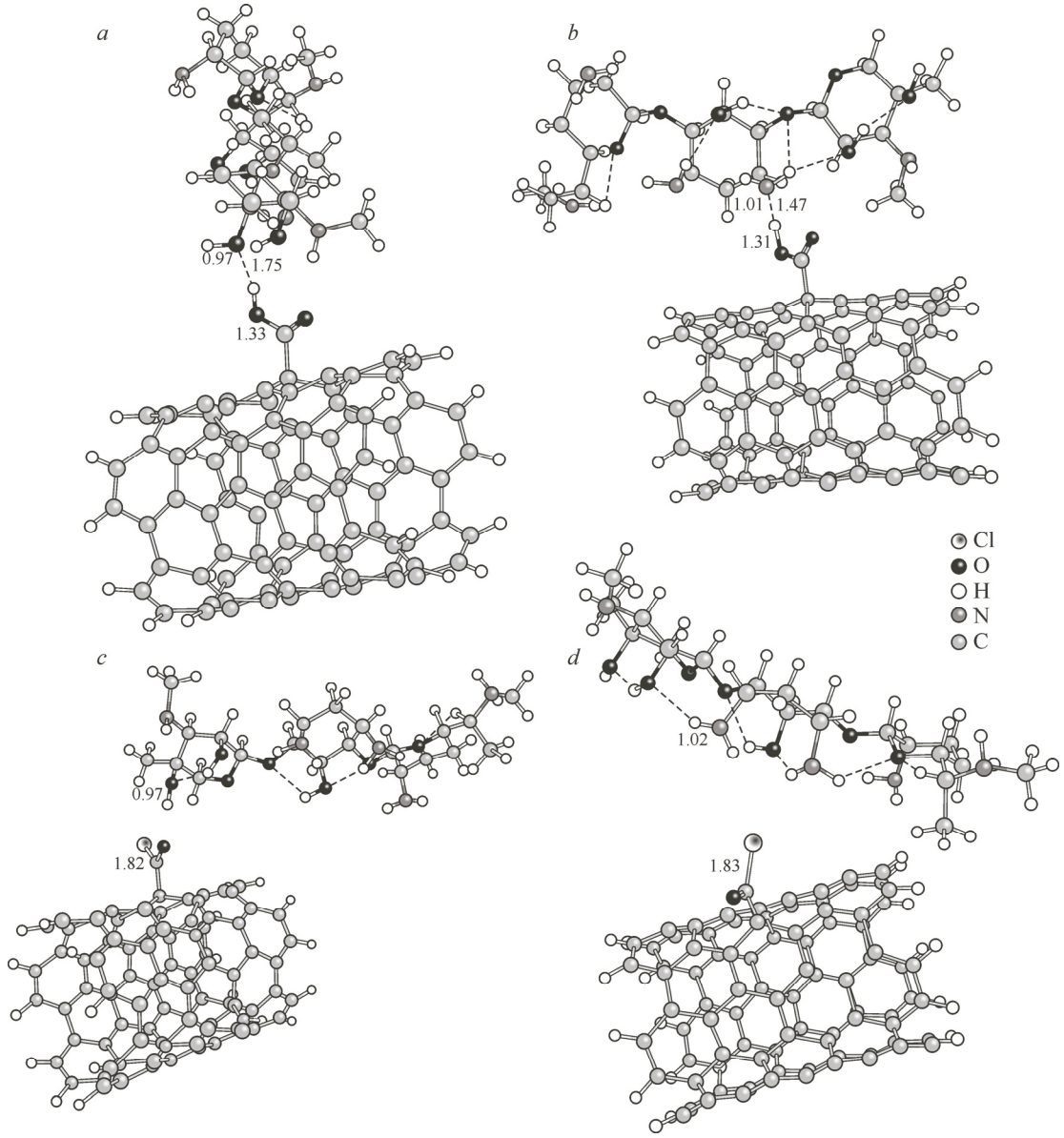

Fig. 2. Optimized structures of RNCOOH/OH (*a*), RNCOOH/NH (*b*), RNCOCl/OH (*c*), and RNCOCl/NH (*d*)

The chemical potential (μ), which shows the escape tendency of an electron from the equilibrium, is defined as follows:

$$\mu = -(I + A) / 2, \quad (2)$$

where $I = -E_{HOMO}$ is the ionization potential and $A = -E_{LUMO}$ is the electron affinity of the molecule.

The global hardness (η) shows the resistance of one chemical species against the change in its electronic structure (Eq. 3). An increase in η causes an increase in the stability and a decrease in reactivity

$$\eta = (I - A) / 2. \quad (3)$$

The electrophilicity index (ω) was defined by Parr as follows [20]:

$$\omega = \mu^2 / 2\eta. \quad (4)$$

Tabel 1 represents the values of quantum molecular descriptors calculated for the optimized geometries of gentamicin, COOH (COCl) functionalized SWCNT, RNCOOH/OH (NH) and RNCOCl/OH (NH). In this table, apart from quantum molecular descriptors, E_g (HOMO-LUMO energy gap) was also presented. E_g notably shows a more stable system. Formally, the HOMO-LUMO gap is the gap between the α-HOMO and β-LUMO. However, a given pair of α- and β-spin orbitals is almost identical in terms of their density distribution and can be thought of as describing the corresponding two-electron orbital. Thus, the α-HOMO-α-LUMO gap should be considered to be the physically significant HOMO-LUMO gap in these systems [21].

According to the Table 1 data, η, I, and E_g related to the gentamicin drug are higher than those for RNCOOH/OH (NH) and RNCOCl/OH (NH), showing that the stability of gentamicin decreases in the presence of COOH (COCl) functionalized SWCNT and its reactivity increases. Also, in confirmation of the previous issue, it is observed that μ of gentamicin becomes more positive in the presence of COOH (COCl) functionalized SWCNT.

ω of gentamicin increases in the presence of COOH (COCl) functionalized SWCNT, showing that gentamicin acts as an electron acceptor. This issue is confirmed through the calculation of a partial number of electrons transferred from gentamicin to SWCNT (ΔN)

$$\Delta N = \mu_{NT(NTCOOH)} - \mu_{GEN} / 2(\eta_{GEN} - \eta_{NT(NTCOOH)}). \quad (5)$$

ΔN is 0.18 and 0.16 for NCOOH and NCOCl, respectively. A positive value of ΔN indicates that the charge flows from the nanotube to gentamicin.

A comparison between RNCOOH/OH (NH) and RNCOCl/OH (NH) in Table 1 shows that the second is more reactive, and amino and hyroxyl groups are prepared for attacking the carbon atom of COCl (COOH) with transferring their protons to the Cl (OH) group. We investigated these four possible mechanisms.

Scheme 1 shows the mechanism of covalent functionalization of GEN onto COOH functionalized carbon nanotube (COOH mechanism), where K_1 and K_1' are the equilibrium constants and k_1 is the rate

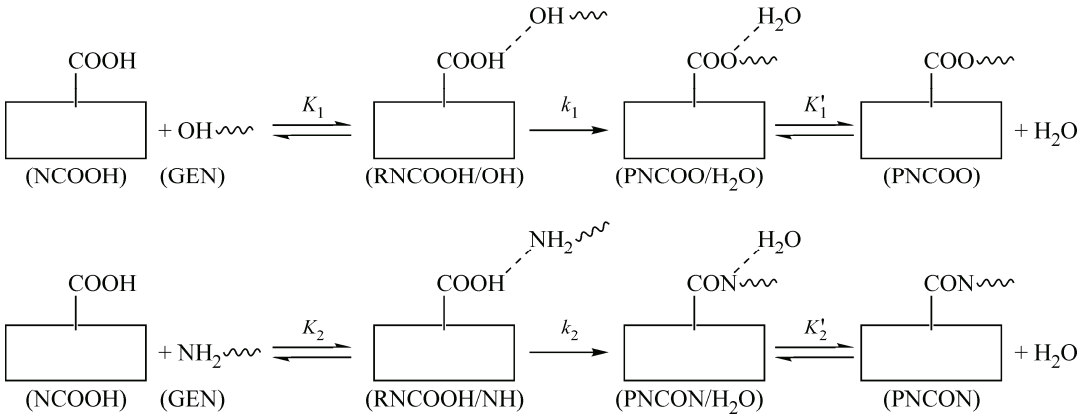

Scheme 1. Mechanism of covalent functionalization of GEN onto the COOH functionalized carbon nanotube

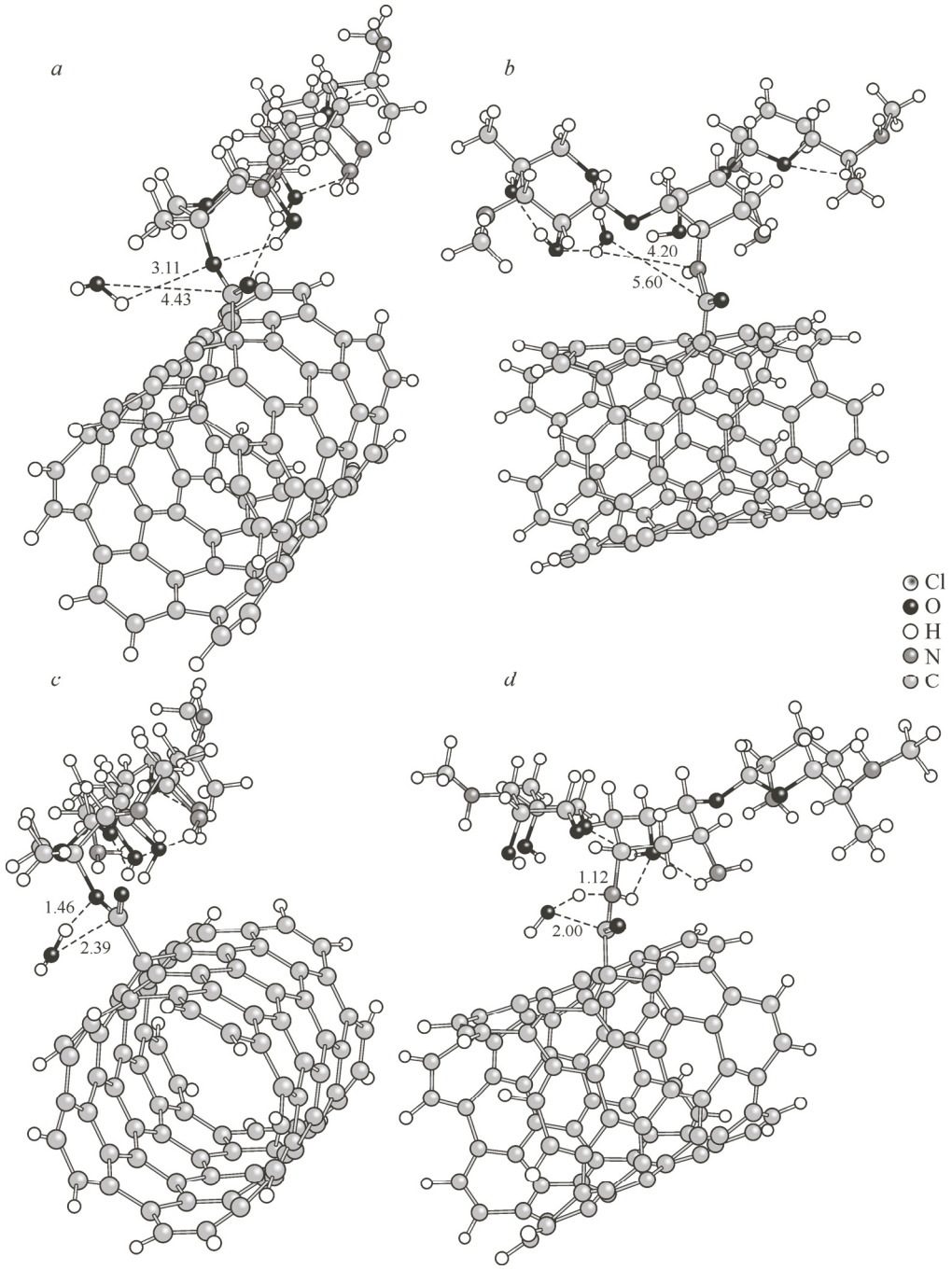

Fig. 3. Optimized structure of PNCOO/H_2O (*a*), PNCON/H_2O (*b*), TS_{k1} (*c*), and TS_{k2} (*d*)

constant. In the COOH mechanism, RNCOOH/OH and RNCOOH/NH are converted into the PNCOO/H_2O (k_1 pathway) and PNCON/H_2O (k_2 pathway) products by losing H_2O, respectively.

As shown in Scheme 1, the COOH mechanism corresponds to a replacement of OH from NCOOH by O (NH) of GEN to give the PNCOO (PNCON) product. In order to find the transition states of k_1 and k_2 pathways (Scheme 1), the PNCOO and PNCON products in the vicinity of H_2O should be optimized (PNCOO/H_2O and PNCON/H_2O). The optimized structures of PNCOO/H_2O and PNCON/H_2O have been depicted in Fig. 3, *a* and *b*, respectively.

Considering the RNCOOH/OH reactant and the PNCOO/H_2O product, the transition state of k_1 step is obtained, which we call TS_{k_1}. Fig. 3, *c* presents the optimized structures of TS_{k_1}. As seen from

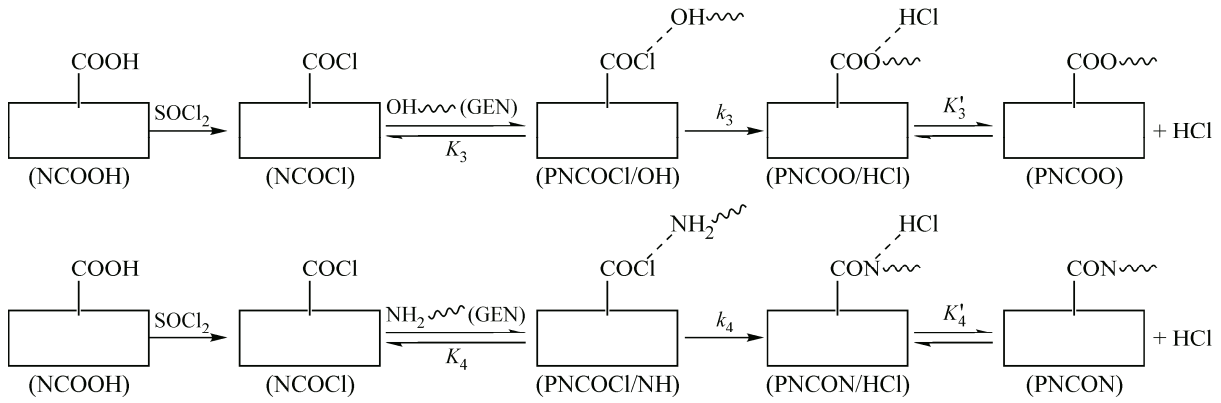

Scheme 2. Mechanism of covalent functionalization of GEN onto a COOH functionalized carbon nanotube

Figs. 2, *a*, 3, *a* and *c*, the C—O and O—H bond lengths increase (decrease) from 1.33 Å and 0.97 Å (4.43 Å and 3.11 Å) for RNCOOH/OH (PNCOO/H_2O) to 2.39 Å and 1.46 Å for TS_{k_1}, respectively. The activation energy (E_a) related to the k_1 pathway is 238.38 kJ·mol^{-1}.

Using the RNCOOH/NH reactant and the PNCON/H_2O product, the transition state of the k_2 step is obtained, which we call TS_{k_2}. Fig. 3, *d* presents the optimized structure of TS_{k_2}. As seen from Figs. 2, *b*, 3, *b* and *d*, the C—O and N—H bond lengths increase (decrease) from 1.31 Å and 1.01 Å (5.60 Å and 4.20 Å) for RNCOOH/NH (PNCON/H_2O) to 2.00 Å and 1.12 Å for TS_{k_2}, respectively. The activation energy (E_a) related to the k_2 pathway is 203.42 kJ·mol^{-1}.

Another method for the study of covalent adsorption of drugs onto a COCl functionalized carbon nanotube is shown in Scheme 2 (COCl mechanism) [22]. In this method, the carboxylic acid functionalized nanotube was firstly converted into alkyl chloride by treating with $SOCl_2$ (NCOCl). GEN then reacts with alkyl chloride to form an ester bond (PNCOO/HCl) or an amide bond (PNCON/HCl).

The COCl pathway commences with the attack of OH (NH2) of GEN to Cl in NCOCl. The optimized structures of PNCOO/HCl and PNCON/HCl products are shown in Fig. 4, *a* and *b*, respectively. Using RNCOCl/OH and PNCOO/HCl (RNCOCl/NH and PNCON/HCl), a transition state is obtained, which we call TS_{k_3} (TS_{k_4}). The optimized structures of TS_{k_3} and TS_{k_4} are presented in Fig. 4, *c* and *d*, respectively.

As seen from Figs. 2, *c*, 4, *a* and *c*, the C—Cl and O—H bond lengths increase (decrease) from 1.82 Å and 0.97 Å (5.61 Å and 3.80 Å) for RNCOCl/OH (PNCOO/HCl) to 3.38 Å and 1.06 Å for TS_{k_3}, respectively. The activation energy (E_a) related to the k_3 pathway is 83.48 kJ·mol^{-1}. As seen from Figs. 2, *d*, 4, *b* and *d*, the C—Cl and N—H bond lengths increase (decrease) from 1.83 Å and 1.02 Å (3.76 Å and 2.68 Å) for RNCOCl/NH (PNCON/HCl) to 2.74 Å and 1.17 Å for TS_{k_4}, respectively. The activation energy (E_a) related to the k_4 pathway is 47.51 kJ·mol^{-1}.

Fig. 5 shows the energy profile for the COOH and COCl mechanisms. E_a for k_3 and k_4 pathways are lower than that for k_1 and k_2 pathways by 154.9 kJ·mol^{-1} and 155.91 kJ·mol^{-1}, respectively. Amongst k_3 and k_4 pathways, the contribution of the k_4 pathway is higher. Therefore, it is predicted that cross linkers such as $SOCl_2$ and $POCl_3$ are required for the covalent functionalization of gentamicin onto COOH functionalized carbon nanotubes.

Both reactions involve the nucleophilic substitution at a carbonyl carbon atom. Such reactions are generally understood to proceed via a tetrahedral intermediate. To investigate whether this matter applies as well to functionalized SWCNTs or not, a tetrahedral intermediate was designed. Beginning with the initial structure of this intermediate, an ultimately optimized structure was obtained, which is similar to RNCOCl/OH or RNCOCl/NH, meaning that the tetrahedral intermediate could not be formed, being probably due to the steric and electronic effects of functionalized SWCNTs.

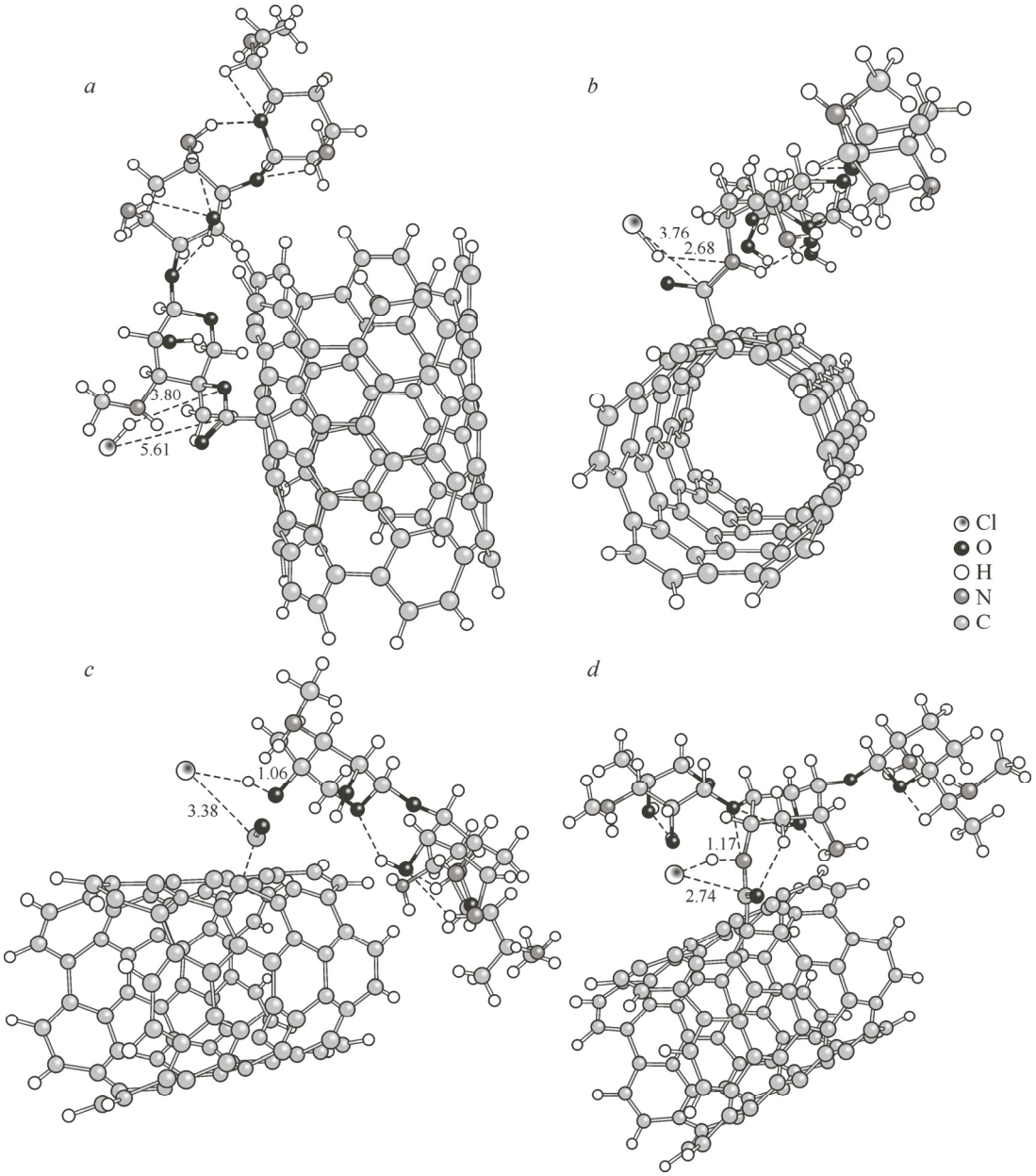

Fig. 4. Optimized structures of PNCOO/HCl (*a*), PNCON/HCl (*b*), TS_{k3} (*c*), TS_{k4} (*d*)

CONCLUSIONS

The mechanisms of adsorption of gentamicin in the presence of COOH (NCOOH) and COCl (NCOCl) functionalized carbon nanotubes have been studied in detail. Four possible modes of the noncovalent interaction of gentamicin onto NCOOH and NCOCl were investigated. There are two possibilities for the formation of hydrogen bonds between gentamicin and NCOOH (NCOCl). For the first possibility, gentamicin is interacted with NCOOH (NCOCl) through amino groups (NCOOH(OCl)/NH), and for the second one through hydroxyl groups (NCOOH(OCl)/OH). The binding energies of NCOOCl are lower than those for NCOOH, indicating that NCOOH/OH(NH) configurations are stabilized. The global hardness and the HOMO-LUMO energy gap of gentamicin are higher than those of NCOOH(OCl)/OH(NH), showing that the stability of gentamicin decreases in the presence of NCOOH(Cl) and its reactivity increases.

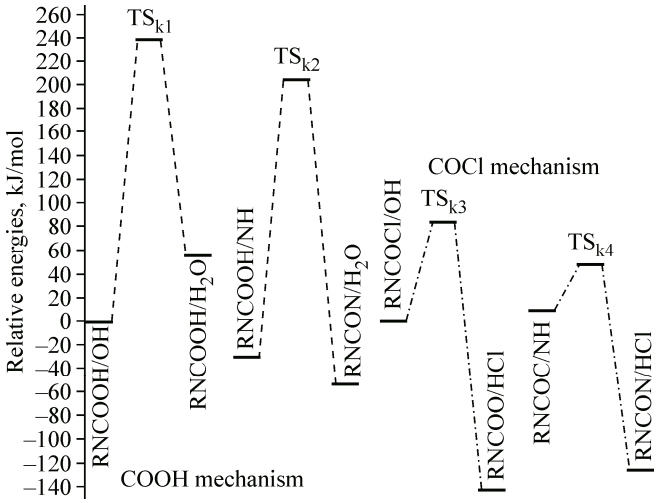

Fig. 5. Energy profile for the COOH and COCl mechanisms

There are two mechanisms for the covalent functionalization between NCOOH(Cl) and gentamicin. For the first mechanism, the carbon nanotube is bonded to gentamicin through the COOH group (COOH mechanism) and for the second one through the COCl group (COCl mechanism). The COCl mechanism has an energy barrier lower than that of the COOH mechanism. Amongst OH (k_3) and NH (k_4) pathways in the COCl mechanism, the contribution of the NH pathway is higher.

COMPUTATIONAL METHODS

All of the present calculations have been performed at the UB3LYP [23—25] hybrid density functional level and 6-31G(*d*,*p*) basis sets using the GAUSSIAN 03 package [26]. The solvent explicitly or implicitly plays an important role in chemical reactions [27—33]. The implicit effects of the solvent was considered using the polarized continuum model (PCM) [34, 35]. In the PCM method, the molecular cavity is made up of the union of interlocking atomic spheres.

All degrees of freedom for all geometries were optimized in the solution phase (water). The calculations were performed on gentamicin, COOH and COCl functionalized armchair (5,5) SWCNT comprising 114 atoms (10 Å) with the ends terminated by hydrogen atoms. In the optimization of the structures, no use has been made of approximations such as ONIOM [36] and in spite of a high computational cost, we preferred to obtain the results with good accuracy.

Acknowledgments. We thank the Research Center for Animal Development Applied Biology for allocation of computer time.

REFERENCES

1. *Popat K.C., Eltgroth M., LaTempa T.J., Grimes C.A., Desai T.A.* // Biomaterials. – 2007. – **28**. – P. 4880 – 4888.
2. *Tomalia D., Reyna L., Svenson S.* // Biochem. Soc. Trans. – 2007. – **35**. – P. 61.
3. *Chonn A., Cullis P.R.* // Curr. Opin. Biotechnol. – 1995. – **6**. – P. 698 – 708.
4. *Allen T.M., Cullis P.R.* // Science. – 2004. – **303**. – P. 1818 – 1822.
5. *Prato M., Kostarelos K., Bianco A.* // Acc. Chem. Res. – 2007. – **41**. – P. 60 – 68.
6. *Wong S., Yoong S.L., Jagusiak A., Panczyk T., Ho H.K., Ang W.H., Pastorin G.* // Adv. Drug. Deliv. Rev. – 2013. – **65**. – P. 1964 – 2015.
7. *Sharifi S., Hashemi M.M., Mosslemin M., Mollaamin F.* // J. Comput. Theor. Nanosci. – 2014. – **11**. – P. 1178 – 1183.
8. *Hosni Z., Bessrour R., Tangour B.* // J. Comput. Theor. Nanosci. – 2014. – **11**. – P. 318 – 323.
9. *Saikia N., Deka R.C.* // J. Mol. Model. – 2013. – **19**. – P. 215 – 226.
10. *Prajongtat P., Suramitr S., Gleeson M.P., Mitsuke K., Hannongbua S.* // Monatsh. Chem. – 2013. – **144**. – P. 925 – 935.

11. *Lin Y., Allard L.F., Sun Y.-P.* // J. Phys. Chem. B. – 2004. – **108**. – P. 3760 – 3764.
12. *Azimov J., Mamatkulov S., Turaeva N., Oxengendler B., Rashidova S.S.* // J. Struct. Chem. – 2012. – **53**. – P. 829 – 834.
13. *Star A., Liu Y., Grant K., Ridvan L., Stoddart J.F., Steuerman D.W., Diehl M.R., Boukai A., Heath J.R.* // Macromolecules. – 2003. – **36**. – P. 553 – 560.
14. *Beheshtian J., Peyghan A.A., Bagheri Z.* // Monatsh. Chem. – 2012. – **143**. – P. 1623 – 1626.
15. *Canto G., Martínez-Guerra E., Takeuchi N.* // Comp. Mater. Sci. – 2008. – **42**. – P. 322 – 328.
16. *Dovbeshko G., Fesenko O., Obraztsova E., Allakhverdiev K., Kaja A.* // J. Struct. Chem. – 2009. – **50**. – P. 954 – 961.
17. *Rajarajeswari M., Iyakutti K., Kawazoe Y.* // J. Mol. Model. – 2012. – **18**. – P. 771 – 781.
18. *Baei M.T., Peyghan A.A., Moghimi M.* // Monatsh. Chem. – 2012. – **143**. – P. 1463 – 1470.
19. *Li H., He J., Zhao Y., Wang G., Wei Q.* // J. Inorg. Organomet. Polym. – 2011. – **21**. – P. 890 – 892.
20. *Parr R.G., v. Szentpaly L., Liu S.* // J. Am. Chem. Soc. – 1999. – **121**. – P. 1922 – 1924.
21. *Fehir J., Richard J., McCusker J.K.* // J. Phys. Chem. A. – 2009. – **113**. – P. 9249 – 9260.
22. *Lin T., Bajpai V., Ji T., Dai L.* // Aust. J. Chem. – 2003. – **56**. – P. 635 – 651.
23. *Becke A.D.* // Phys. Rev. A. – 1988. – **38**. – P. 3098.
24. *Becke A.D.* // J. Chem. Phys. – 1993. – **98**. – P. 5648 – 5652.
25. *Lee C., Yang W., Parr R.G.* // Phys. Rev. B. – 1988. – **37**. – P. 785.
26. *Frisch M.J., Trucks G.W., Schlegel H.B., Scuseria G.E., Robb M.A., Cheeseman J.R., Scalman G., Barone V., Mennucci B., Petersson G.A., Nakatsuji H., Caricato M., Li X., Hratchian H.P., Izmaylov A.F., Bloino J., Zheng G., Sonnenberg J.L., Hada M., Ehara M., Toyota K., Fukuda R., Hasegawa J., Ishida M., Nakajima T., Honda Y., Kitao O., Nakai H., Vreven T., Montgomery J.A. Jr., Peralta J.E., Ogliaro F., Bearpark M., Heyd J.J., Brothers E., Kudin K.N., Staroverov V.N., Kobayashi R., Normand J., Raghavachari K., Rendell A., Burant J.C., Iyengar S.S., Tomasi J., Cossi M., Rega N., Millam J.M., Klene M., Knox J.E., Cross J.B., Bakken V., Adamo C., Jaramillo J., Gomperts R., Stratmann R.E., Yazyev O., Austin A.J., Cammi R., Pomelli C., Ochterski J.W., Martin R.L., Morokuma K., Zakrzewski V.G., Voth G.A., Salvador P., Dannenberg J.J., Dapprich S., Daniels A.D., Farkas O., Foresman J.B., Ortiz J.V., Cioslowski J., Fox D.J.* In: Gaussian Inc., Wallingford CT, 2009.
27. *Hooman Vahidi S., Morsali A., Beyramabadi S.A.* // Comput. Theor. Chem. – 2012. – **994**. – P. 41 – 46.
28. *Beyramabadi S.A., Morsali A., Shams A.* // J. Struct. Chem. – 2015. – **56**. – P. 243 – 249.
29. *Morsali A., Hoseinzade F., Akbari A., Beyramabadi S.A., Ghiasi R.* // J. Solution Chem. – 2013. – **42**. – P. 1902 – 1911.
30. *Beyramabadi S.A., Morsali A., Vahidi S.H., Khoshkholgh M., Esmaeili A.* // J. Struct. Chem. – 2012. – **53**. – P. 460 – 467.
31. *Beyramabadi S.A., Eshtiagh-Hosseini H., Housaindokht M.R., Morsali A.* // Organometallics. – 2007. – **27**. – P. 72 – 79.
32. *Eshtiagh-Hosseini H., Beyramabadi S.A., Mirzaei M., Morsali A., Salimi A., Naseri M.* // J. Struct. Chem. – 2013. – **54**. – P. 1063 – 1069.
33. *Morsali A.* // Int. J. Chem. Kinet. – 2015. – **47**. – P. 73 – 81.
34. *Cammi R., Tomasi J.* // J. Comput. Chem. – 1995. – **16**. – P. 1449 – 1458.
35. *Tomasi J., Persico M.* // Chem. Rev. – 1994. – **94**. – P. 2027 – 2094.
36. *Dapprich S., Komáromi I., Byun K.S., Morokuma K., Frisch M.J.* // J. Mol. Struct.: THEOCHEM. – 1999. – **461**. – P. 1 – 21.